recycling

MDPI

Article

Multi-Assay Characterization of an LED Recycler Feedstock for Economic and Environmental Valuation of Critical Metals

Mehdi Golzar-Ahmadi * and Maria Holuszko

NBK Institute of Mining Engineering, University of British Columbia, Vancouver, BC V6T 1Z4, Canada; maria.holuszko@ubc.ca

* Correspondence: mehdi.ahmadi@ubc.ca

Abstract

Urban mining is gaining importance as demand for critical metals continues to rise. Waste light-emitting diode (LED) lamps are a valuable secondary source of gallium, rare earth elements, precious metals, and base metals, yet accurately quantifying these metals remains challenging. In this work, various LED waste streams from a lamp recycler were subjected to critical metal characterization. The strengths and weaknesses of established metal assay techniques were evaluated to advance the determination of gallium, rare earth elements (Ho, Lu, Tb, Y, Er, Nd, Ce), and precious metals (Au, Ag, Pt, Pd) in LED waste. Metal assays, including alkaline fusion, four-acid digestion, aqua regia, a fire assay, and energy-dispersive X-ray fluorescence, were compared, and precision was assessed using a newly created LED lamp reference material and OREAS465. A metal-analysis-driven approach was developed to quantify the reduction in mining through recycling LED lamps using the rock-to-metal ratio metric. The economic value of LED waste streams, together with their recyclability and grindability, was assessed. The results indicate that LED strips can contain up to 147,484 g/t Cu, 452 g/t Ga, 367 g/t Lu, 89 g/t Tb, and 95 g/t of precious metals. Recycling one tonne of waste LEDs can offset mining 75.5 tonnes of rock and primary ore. The estimated economic value of mixed LED waste was USD 3351 per tonne, increasing to USD 4089 per tonne after physical separation. The results demonstrate the importance of robust analytical methods for accurate metal accounting and provide a stronger foundation for assessing the recycling potential of LED waste.

Keywords: recycling; e-waste; light-emitting diode; urban mining; gallium; rare earth elements; precious metals

Check for updates

Academic Editor: Francesco Ferella

Received: 9 June 2026
Revised: 5 July 2026
Accepted: 7 July 2026
Published: 8 July 2026

Copyright: © 2026 by the authors. Licensee MDPI, Basel, Switzerland. This article is an open access article distributed under the terms and conditions of the Creative Commons Attribution (CC BY) license.

1. Introduction

The energy efficiency and flexible design of LED lamps have led to their rapid growth in the lighting industry [1,2]. In British Columbia, Canada, the annual sale of LED lamps increased 27-fold, reaching 12 million units in 2020 [3,4]. The technology used in most LED light bulbs and tube LED lamps is phosphor-converted white LED [5]. A tube lamp or light bulb is composed of components such as the LED module, heat sink, driver, and diffuser [6] (Figure 1). Gallium nitride (GaN) and indium gallium nitride (InGaN) are primarily used as semiconductor materials in blue LEDs with sapphire (α-Al_2O_3), Si or SiC as the substrate [6,7]. The phosphor light converter in these lamps is 87% Si, 10% yttrium aluminum garnet (YAG, $Y_3Al_5O_{12}$) doped with Ce^{3+} ($Y_{0.98}Ce_{0.02}(Al_5O_{12})$) and 3% $Ca_{0.98}Eu_{0.02}AlSiN_3$ (CASN) [8] (Figure 1). Elements like gold (Au), palladium (Pd), silver

(Ag), and copper (Cu) are utilized in LED lamps as electrical contacts (such as Au-Ag, Cu-Pd, Ag-Pd wire bonding) [6,7,9,10]. Additionally, lead (Pb) and tin (Sn) are used as solders, and aluminum (Al) is used to help with heat dissipation [7,11]. The lens contains hazardous organic compounds, including epoxy resins and brominated flame retardants [12].

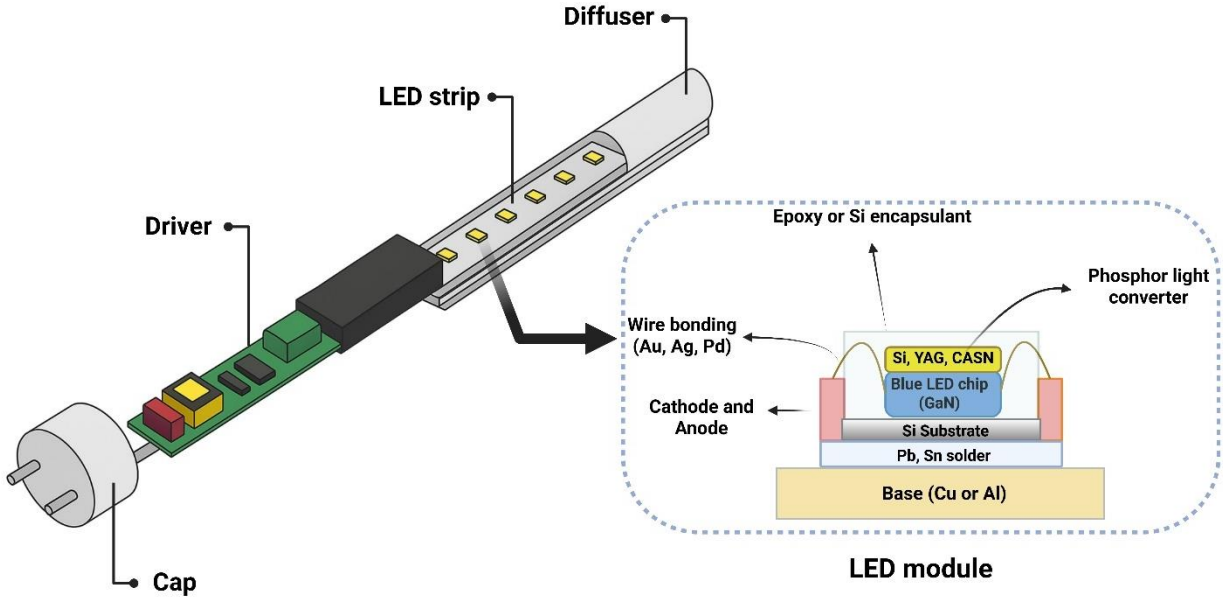


Figure 1. Schematic illustration of a tube LED lamp and an LED module on the strip component.

LED lamps contain nearly ten times more Ga than the primary resource (500–600 g/t on average against 60 g/t in bauxite), with notable rare earth element (REE), Ag, Au, Sn, and Cu content (Table 1). These critical metals are of paramount importance for several industries (Figure 2). A recent report from the United State Geological Survey (USGS) estimates potential losses of $2B, $1.8B and $1.4B USD in the US gross domestic product (GDP) due to supply chain issues for lutetium (Lu), terbium (Tb), and Ga, respectively, which affect semiconductor manufacturing and the illumination industry [13].

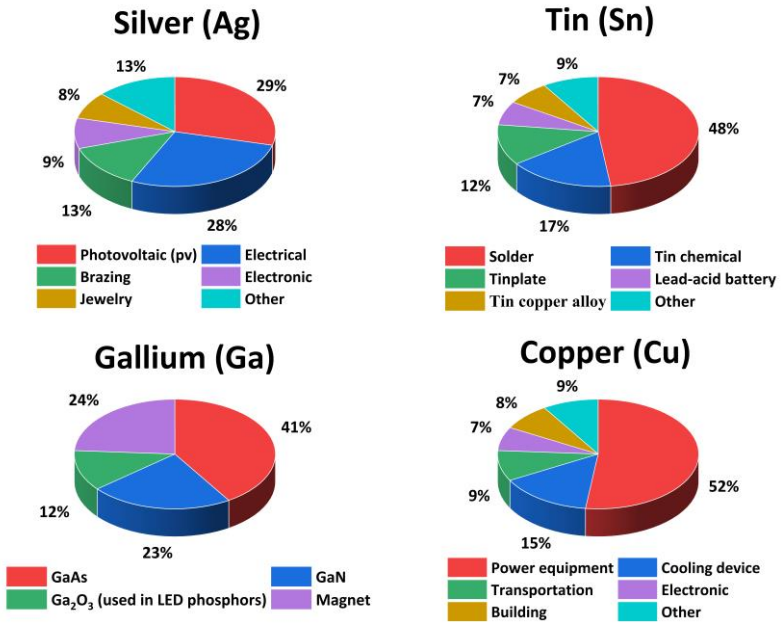


Figure 2. *Cont.*

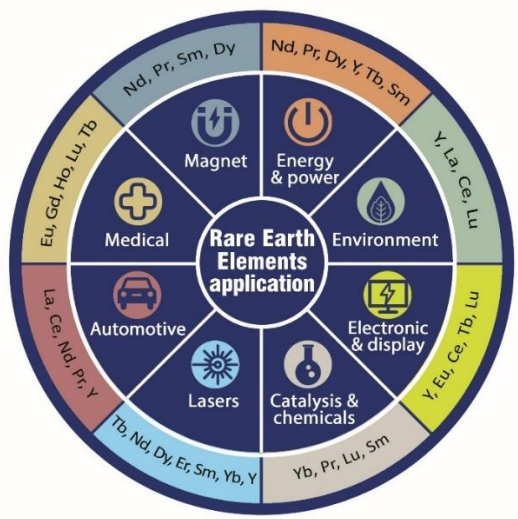


Figure 2. Industrial application of critical metals found in LED lamps in diverse technology fields (based on Chinese industry data) [10,13,14].

Rock-to-metal ratio (RMR) is the amount of waste rock and ore excavation required to obtain a refined metal [15]. This metric can serve as a tool to perceive the environmental impact of rock excavation in mining and understand potential environmental benefits from recycling. According to the RMR metric, recycling 1 kg of gold, platinum, palladium, and gallium from secondary sources can prevent the mining of 3000, 834, 688, and 15 tonnes of ore and waste rock, respectively [15].

Although LED lamps contain significant concentrations of critical metals, establishing a reliable recycling route remains challenging [16]. A central limitation is the absence of characterization methodologies that accurately reflect real recycling feedstocks. Existing studies have largely focused on specific LED components or lamp types, which do not represent the heterogeneous mixtures processed by recyclers (Table 1). As a result, the overall critical metal content of LED recycling feedstock remains poorly understood.

Furthermore, previous characterization efforts have frequently failed to quantify refractory elements, such as rare earth elements (REEs), gallium, and platinum-group metals (PGMs), with sufficient accuracy [17]. The strong chemical stability of LED phosphors and gallium nitride structures limits the effectiveness of commonly used digestion methods, including aqua regia and nitric acid-based microwave digestion, leading to systematic underestimation of metal concentrations [7,16,18,19]. In contrast, aggressive digestion techniques such as alkaline fusion and four-acid digestion have demonstrated near-total dissolution of refractory matrices and proven effectiveness in a range of e-waste streams such as fluorescent lamp phosphors, printed circuit boards (PCBs), magnets, and lithium manganese iron phosphate (LMFP) batteries [20–28]. However, the comparative performance of alkaline fusion and four-acid digestion methods for characterizing LED waste have not been rigorously evaluated.

An additional and critical knowledge gap is the lack of suitable reference materials for LED waste. The absence of matrix-matched reference materials prevents verification of digestion completeness and comparability across analytical methods [29]. This limitation can lead to underreported metal concentrations and undervaluation of the economic potential of LED recycling.

In this paper, the aforementioned gaps were addressed by (*i*) characterization of mixed LED feedstock from an active lamp recycler; (*ii*) expansion of the quantified metal suite to include Ga, REEs, PGMs, and precious metals across multiple LED components and recycler samples by using sodium peroxide fusion, four-acid digestion and the fire assay;

(*iii*) comparison of a newly developed LED reference material and a certified ore reference material for metal assay quality control; (*iv*) economic assessment of recoverable metals from waste LEDs; and (*v*) applying the RMR metric to quantify the environmental benefits of LED recycling.

To our knowledge, this is the first study to compare diverse metal analysis methods for characterizing LED recycler feedstock before and after physical separation, thereby providing a more realistic assessment of the value contained in LED lamps. In addition, we developed a metal-analysis-driven approach to demonstrate the potential of LED recycling to reduce ore excavation, highlighting the role of urban mining in lowering carbon emissions across the metal supply chain.

Table 1. Metal composition of different LEDs characterized by previous research (mg/kg).

LED Type	Ga	In	Al	Sn	Fe	As	Pb	Au	Pt	Pd	Ag	Cu	Tb	Nd	Y	Lu	Ce	Ref.
MT LED	-	-	11%	-	-	66	-	348	-	-	384	9.4%	-	-	20	-	16	[18]
MT LED	-	-	22%	-	3%	50	300	-	-	-	30	2%	-	-	-	-	-	[19]
SMD LED	22	-	-	-	65.7%	-	-	-	-	-	-	1.3%	-	-	-	-	-	[30]
SMD LED	41	21	-	-	-	9	-	-	-	-	805	-	-	-	-	-	-	[31]
SMD LED	-	-	-	-	-	-	-	934	-	110	5262	-	-	-	9372	6381	284	[6]
SMD LED	1231	-	9319	-	1.3%	-	4992	192	-	-	139	62.8%	-	-	-	-	-	[32]
SMD LED	72	-	2552	-	1.3%	1	12	1204	-	-	337	60.5%	-	-	7	-	2	[16]
Pin-type LED	401	124	360	1.2%	32%	130	300	60	-	-	1800	5400	-	-	-	-	-	[33]
Pin-type LED	79	-	156	-	39.8%	84	-	30	-	-	336	2948	-	-	-	-	-	[34]
LED module	700	-	2860	10.3%	-	-	8.3%	-	-	-	1660	50.4%	-	-	4040	-	7	[7]
LED module	259	-	3290	11.1%	28.5%	-	6%	150	-	-	1590	21.5%	-	-	5070	-	90	[17]
LED module	520	-	2120	13.8%	270	-	-	180	-	-	2390	35%	-	-	1.4%	-	200	[17]
LED module	840	-	1940	6.8%	4800	-	1%	540	-	-	7180	59%	-	-	-	-	-	[35]
LED module	3810	-	2520	10.9%	7410	-	-	520	-	-	4820	54.6%	-	-	-	-	-	[35]
LED module	12,100	1100	-	-	-	-	-	1210	-	-	780	-	-	-	4590	-	120	[9]

-: Not detected; MT: mixed-type; SMD: surface-mounted device.

2. Materials and Methods

2.1. Sample Preparation

Two tube LED lamp models (LED 12T8 and LED 15T8, Philips, Amsterdam, The Netherlands) were selected from recycling feedstock for dismantling and metal analysis. Moreover, shredded mixed-type LED lamp samples were obtained from the industrial recycling process in BC, Canada, before and after the physical separation stage. The sample collected prior to separation was designated as mixed LED before separation (MLBS), representing the untreated shredded mixed LED feed. The sample collected after separation was designated as mixed LED after separation (MLAS), representing the physically processed fraction remaining after separation of selected components/materials. Following the disassembly of both tube LED models, the LED drivers (designated as D12 and D15) and strips (designated as S12 and S15) were cut into smaller pieces to facilitate fine crushing. Additionally, pre-shredded industrial samples (MLBS and MLAS) underwent subsampling using a Gilson Precision Splitter (Lewis Center, Ohio, USA). A cryomill (SPEX Sample Prep 6875 Freezer/mill, Metuchen, NJ, USA) and a jaw crusher (BICO Inc., Burbank, CA, USA) were used to crush the LED samples. However, due to their inefficiency, a ring

mill was employed for grinding stage (BICO Inc., Burbank, CA, USA). A more detailed grinding procedure is provided in Supplementary Text S1. Three different size fractions (−75, −150, and +150 μm) were generated using a sieve shaker for further metal assay.

2.2. Metal Assays

2.2.1. Alkaline Fusion (AF) Procedure

A portion of dried and pulverized LED samples (0.1 g) was added to an alkaline fusion agent (1 g sodium peroxide) and thoroughly mixed using a glass rod in a zirconium crucible. Next, alkaline fusion was performed at 750 °C using Claisse TheOx® Electric Fusion Instrument (Malvern PANalytical, Worcestershire, UK). After fusion, the crucibles were cooled, and approximately 50 mL of distilled water was added to the fused product. For digestion, 10 mL concentrated nitric acid (HNO_3) and 2 g tartaric acid ($C_4H_6O_6$) were used. Thereafter, the solution was transferred into a 100 mL volumetric flask, made up to 100 mL with distilled water, and analyzed by inductively coupled plasma–mass spectrometer (ICP-MS) (Perkin Elmer (Nexion 1000), Shelton, Connecticut, USA) for REE concentration determination and inductively coupled plasma–optical emission spectrometer (ICP-OES) (Perkin Elmer (Avio 500), Shelton, Connecticut, USA) to measure other metal concentrations. Since the volatilization of Cu and Ag during high-temperature processing of e-waste has already been reported, these elements were excluded from the metal analysis by alkaline fusion [36].

2.2.2. Four-Acid Digestion (4AD) Procedure

A known quantity of dried LED samples (0.5 g) was mixed with 2 mL concentrated HNO_3 in Teflon digestion tubes. After a few minutes, 2 mL of concentrated HCl, 2 mL of $HClO_4$, and 5 mL of HF were added to the solution, and the reaction was allowed to continue for 15 min at room temperature. Subsequently, digestion tubes were placed in a heating block at 100 °C for 30 min, then heated to 185 °C, and digestion continued until the samples were nearly dry. After cooling down the tubes to room temperature, 10 mL of HCl was added to dissolve the residue. Following HCl addition, the tubes were returned to the heating block and maintained at 100 °C for 20 min. Then, the solutions were air-cooled, transferred to 100 mL volumetric flasks, and made up to volume with deionized water. Lastly, samples were analyzed by ICP-OES to measure metal concentrations.

2.2.3. Aqua Regia (AR) Digestion

Initially, an aqua regia solution was prepared by mixing 15 mL of concentrated HCl and 5 mL of HNO_3 in 100 mL beakers. Next, a portion of the sample (0.5 g) was added to the beaker and placed on a magnetic stirrer with a stir bar at 200 °C for 2 h. After cooling, the solution was diluted to 100 mL, and an aliquot was taken for metal analysis by ICP-OES.

2.2.4. Fire Assay (FA) Digestion Procedure

Following cupellation (part of the fire assay process in which the lead button is heated in a cupel to generate a noble metal bead), the bead was flattened and transferred to a digestion tube, and 0.5 mL 50% v/v HNO_3 was added [37]. Each digestion tube was covered with plastic film, placed in a microwave oven at 100% power, and digested for 140 s. After cooling the tubes, 0.5 mL concentrated HCl was added, and the tubes were heated in a microwave at 50% power for 2 min. Then, the samples were removed from the microwave and cooled to room temperature, after which 9 mL of a 3% HNO_3 + 11% HCl solution was added. Lastly, the solution was thoroughly mixed and analyzed by ICP-OES.

The results of digestion–ICP methods were compared with those from an energy-dispersive X-ray fluorescence spectrometer (EDXRF) (Malvern PANalytical Epsilon 4,

Worcestershire, UK) and a portable XRF (pXRF) (OLYMPUS, Vanta™ Workstation, Tokyo, Japan) to assess the accuracy of XRF in determining critical metals in LED waste.

2.3. Quality Assurance and Data Analysis

Certified reference materials and procedural blanks were analyzed alongside samples to ensure analytical accuracy. The reference material for LED samples was prepared by mixing metal powders, including Al, Ca, Cu, Ga, and Ag, representative of the contents of waste LEDs. This methodology has been utilized before to create a reference material for printed circuit boards (PCBs) [29]. Metal powders were sourced from Sigma Aldrich (St. Louis, Missouri, USA) (CAS 215147—5 g 99% Ca, CAS 203319—5 g 99.9995% Ga, CAS GF41668544—100 g 99% Cu, CAS GF59664572—200 g 99% Al, CAS 265500—99.99% Ag). Owing to the high cost and difficulties in obtaining REE powders, a common CRM for REEs in mining (OREAS 465, Bayswater North, Australia) was used to calculate recovery and assess the precision of four-acid digestion and alkaline fusion. The limit of detection (LOD) for each digestion method is presented in the Supplementary File S1.

2.4. Economic Valuation of LED Waste

The market value of the LED recycler feedstock was estimated based on the total metal content of each sample. The total metal content was calculated using Equation (1):

$$Total metal content(mg/kg) = \sum_i^n M_i C_i \quad (1)$$

where M_i is the mass fraction of the sample in size fraction i and C_i is the concentration of target metals in size fraction i.

Based on the concentration of each element per tonne of sample and its corresponding market price, the market value of recoverable metals in each type of LED waste feedstock was then calculated using Equation (2):

$$Market value of LED waste\ (USD/tonne) = \sum_i^n E_i P_i \quad (2)$$

where E_i is the concentration of element i per tonne of sample and P_i is the market price of element i per tonne. Metal prices were taken from https://mineralprices.com/. Additional details of the calculations are provided in the Supplementary File S1.

2.5. Environmental Valuation of LED Waste

The reduction in ore mining achieved through LED lamp recycling was quantified using the rock-to-metal ratio (RMR) for each metal and its concentration in the LED samples. The RMR is expressed as (Equation (3)):

$$RMR = (required\ rock\ excavation\ for\ mining, tonne)/(refined\ metal\ produced, tonne) \quad (3)$$

Accordingly, the avoided rock excavation per tonne of recycled LED waste, assuming complete metal recovery, was determined using the following equation (Equation (4)):

$$Avoided rock excavation(t/t LED waste) = \sum_i^n C_{\mathrm{i}} \times RMR_{\mathrm{i}} \quad (4)$$

where C_i represents the concentration of metal i in a specific LED sample on a tonne basis, and RMR_i represents the corresponding rock-to-metal ratio for that metal. This approach estimates the extent to which recycling LED waste can reduce the need for primary ore extraction.

3. Results and Discussion

3.1. Recyclability of Tube LED Lamps

Although the same company produced both tube LED lamps in this study, they exhibited considerable design differences (Figure S1). The manual disassembly of LED12T8 components, particularly the aluminum base, was relatively easy. The diffuser was made of polycarbonate, and the driver design differed from that of LED15T8 (Figure S1). Given that the average weight of the tube lamp was 200 g, approximately 66 g of clean aluminum could be recovered from the LED12T8 base for direct recycling. The strip and driver of LED12T8, as the two main components that contain high levels of critical metals, accounted for 13% and 2.2% of the total lamp weight, respectively (Figure S1).

In contrast, in the LED15T8 tube lamp, the strip was glued to the aluminum base (Figure S1), making manual separation of the aluminum base difficult. Consequently, the LED15T8 strip was contaminated with significant amounts of Al, resulting in higher energy consumption during grinding and increased chemical use during leaching. Furthermore, the diffuser material in LED15T8 was glass, contributing to a higher weight fraction (70%) than in LED12T8 (44%). The strip and driver constituted 22% and 1.5% of the total lamp weight, respectively (Figure S1). Complete removal of the glass from the LED15T8 strip was also infeasible due to the adhesive used on the strip base (Figure S1).

3.2. Grindability Assessment of LED Samples

The polymeric fraction of e-waste can generate heat during grinding, agglomerate particles, and reduce grinding efficiency [38]. Cryogenic milling has recently been introduced as a grinding method for e-waste to prevent temperature rise during grinding and improve liberation, size, and grain shape [38]. Therefore, a cryomill was used first to grind the LED samples. Although there was negligible sample loss due to the enclosed grinding space, grinding efficiency and capacity were limited. Additionally, more than 15 L of liquid nitrogen was consumed after five grinding cycles on 30 g samples, resulting in a mere 16% wt. passing through the 75 µm screen. Therefore, cryomilling was excluded as the grinding method for LED samples. Primary crushing equipment in mineral processing, such as jaw crushers and cone crushers, showed little to no performance for primary crushing of LED strips and drivers, as observed in other work on crushing PCB samples [38]. Therefore, typical crushing efficiency metrics in mineral processing, such as the crushability index (CI) and impact strength index (ISI), were inapplicable because the standardized methods for measuring these indices require a jaw crusher to obtain particle sizes ranging from 3.18 to 9.52 mm [39]. However, future research into the potential applications of CI, ISI, and the Ball Mill Work Index for e-waste material is highly recommended. These indices are great tools for determining and comparing the grindability of materials. They can help to predict milling energy consumption and design a large-scale milling circuit [40].

In the absence of a standardized metric to evaluate the grindability of different LED samples, the mass of fine material (<75 µm) generated over time during milling was used as an indicator of grinding ease (Figure S2). The brittle structure of the LED12 strip (S12) resulted in the highest grindability among the samples, producing 70.5 g of fine fraction within four minutes of milling, starting with an initial feed mass of 120 g. However, the higher brittleness of the S12 sample also led to greater material loss as dust (10%) compared to 6.6% for S15 (Figure 3). The high Al content of the LED15 strip (S15) contributed to its slower grinding rate compared to S12 (Figure S2) due to its malleable character. Furthermore, the grindability of mixed-type LED samples (MLBS and MLAS) was lower than that of both tube lamp strips (S12 and S15). After four milling cycles, less than 60% of the initial feed mass of the MLBS and MLAS samples passed through a 75 µm sieve, compared with 67.3% and 78.5% for S12 and S15, respectively (Figure 3).

Nevertheless, the grindability trends (Figure S2) indicate that physical separation can enhance grindability and reduce energy consumption by enabling faster and more efficient milling. This improvement can be attributed to the removal of malleable metals such as Al and Fe during the physical separation process of LED lamps.

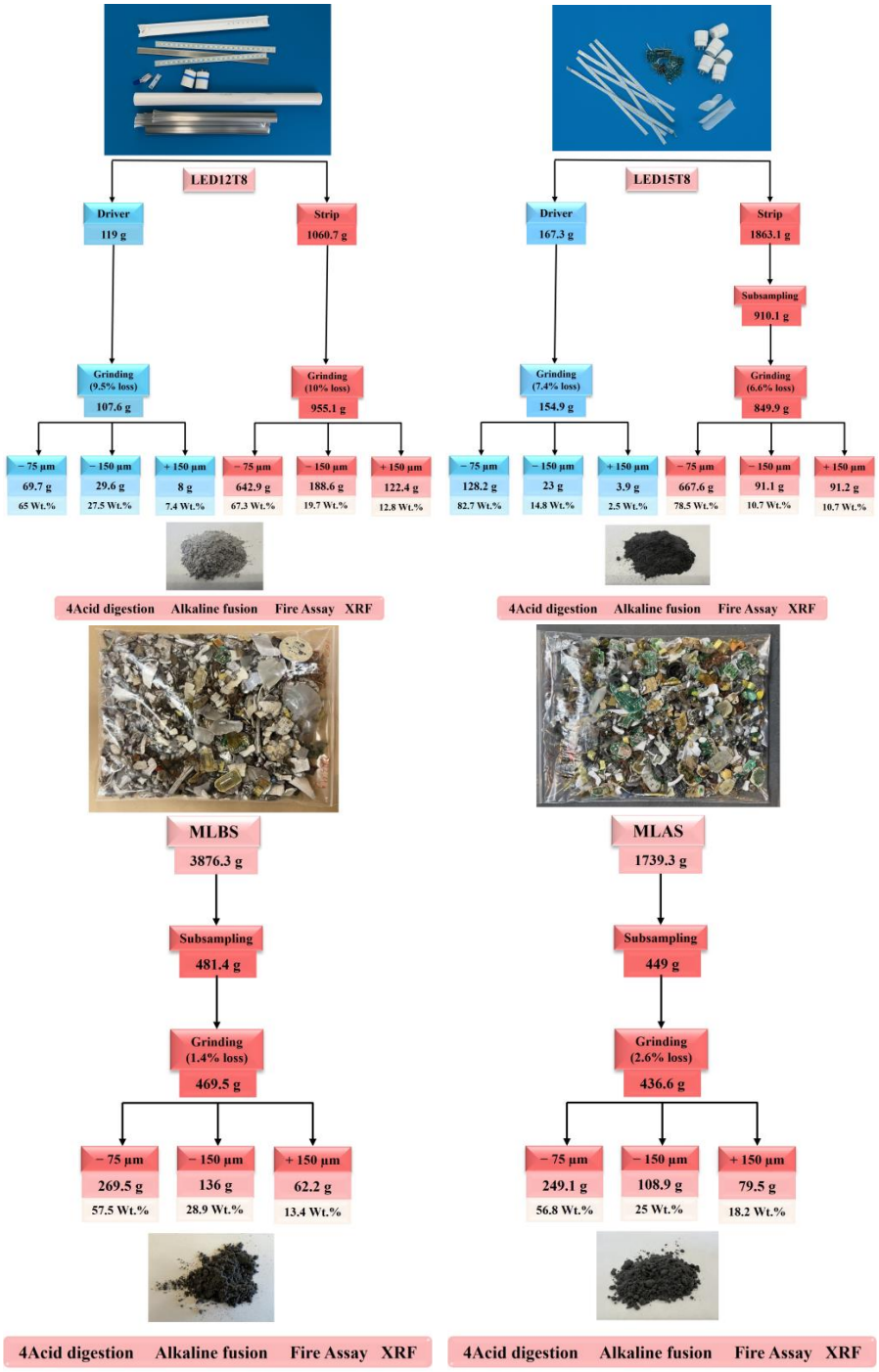


Figure 3. Mass balance of LED samples used in the study.

3.3. Metal Assay of LED Samples

3.3.1. Performance of Digestion and Analytical Methods

As shown in the metal analysis results (Table S1), portable XRF (pXRF) detected the smallest fraction of metals (11.7% compared to 66.3% with EDXRF) and was therefore excluded from further analysis owing to its limited precision. Interestingly, aqua regia (AR) performed better for Al and Fe determination than four-acid digestion (4AD) and

alkaline fusion (AF) (Table 2). Since HNO_3 was used as the first digestion reagent in 4AD and AF, it led to passivation of Al and Fe, and, consequently, sub-determination compared to AR. Previous studies have indicated that utilization of concentrated HNO_3 can passivate various elements (e.g., Al (Equation (5)), Fe, Cr, As, Sb) and precipitate Sn (Equation (6)) [9,41–43]:

$$2Al + 6HNO_3 \rightarrow Al_2O_3 \downarrow + 3H_2O + 6NO_2 \quad (5)$$

$$Sn + 4HNO_3 \rightarrow SnO_2 \downarrow + 2H_2O + 4NO_2 \quad (6)$$

Inferior quantification of Sn and Ti in acid-based digestion methods is due to the formation of an oxide passivation layer (SnO_2, TiO_2), which hinders further solubilization in acidic conditions [37]. Moreover, the volatility of $SnCl_4$ and TiF_4 led to inefficient recovery of Sn and Ti during four-acid digestion, especially in samples with high Sn and Ti contents (S12, D12, D15 in Table 2) [44]. Compounds such as $HClO_4$ during four-acid digestion can generate insoluble Ti, Zr, Nb, and Hf oxides [37,45]. The utilization of the $HF/HClO_4$ mixture in four-acid digestion can lead to volatilization of Si (Equations (7) and (8)), As and Sb and consequently low recovery by ICP (Table 2) [37,45,46]. Historically, accurate determination of Si in rocks has been performed using laborious gravimetric methods [37]. Here, EDXRF demonstrated good accuracy for rapid detection of Si in LED samples (Table 2).

$$SiO_2 + 6HF \rightarrow H_2SiF_6 + 2H_2O \quad (7)$$

$$H_2SiF_6 \rightarrow SiF_4 \uparrow + 2HF \quad (8)$$

Owing to the above reasons, alkaline fusion has been recommended for determining Sn and Ti in solid samples [37,44,45]. The evolution of oxygen during alkaline fusion with sodium peroxide (Na_2O_2) (Equation (9)) can convert Sn and Ti into their (IV) oxides and then generate sodium salts within the fusion melt (e.g., stannate and titanates) (Equation (10)) [47,48]:

$$2Na_2O_2 \rightarrow 2Na_2O + O_2\ (>657\ ^\circ C) \quad (9)$$

$$TiO_2 + Na_2O \rightarrow Na_2TiO_3 \quad (10)$$

Moreover, during water leaching after sodium peroxide fusion, sodium hydroxide and hydrogen peroxide are generated exothermically (Equation (11)). The release of high amounts of heat during this reaction accelerates the decomposition of hydrogen peroxide into water and oxygen (Equation (12)) and leads to the generation of stannate (SnO_3^{2-}) and titanate (TiO_3^{2-}) salts (Equations (13) and (14)) [49].

$$Na_2O_2 + 2H_2O \rightarrow 2NaOH + H_2O_2 \quad (11)$$

$$2Na_2O_2 + 2H_2O \rightarrow 4NaOH + O_2 \quad (12)$$

$$SnO_2 + 2NaOH \rightarrow Na_2SnO_3 + H_2O \quad (13)$$

$$TiO_2 + 2NaOH \rightarrow Na_2TiO_3 + H_2O \quad (14)$$

Table 2. Elemental composition of strip and driver in two different tube lamp models.

Elements (mg/kg)	**S15**				**D15**			**S12**				**D12**		
Assay Method	**EDXRF**	**AR**	**4AD**	**AF**	**EDXRF**	**4AD**	**AF**	**EDXRF**	**AR**	**4AD**	**AF**	**EDXRF**	**4AD**	**AF**
Al	466,458	400,306	227,210	218,130	253,914	4953	5404	55,023	53,175	17,476	17,858	192,461	10,478	10,627
Si	130,801	-*	-	2127	108,919	-	1778	170,834	-	-	4867	127,642	-	3428
Ca	24,048	10,682	13,777	13,860	48,774	20,875	23,544	150,628	84,755	78,503	79,579	78,145	35,215	33,636
Fe	3203	2915	558	242	13,709	8712	7039	4050	1867	1817	2186	14,850	16,102	16,456
Strategic metals														
Cu	29,195	68,847	70,332	-	113,626	186,634	-	65,597	91,013	147,484	-	79,611	124,372	-
Sn	2995	-	-	-	63,901	-	102,417	5797	-	-	6414	87,901	-	123,844
Ti	4815	-	-	-	9885	-	16,160	20,043	-	-	1012	8459	-	1534
Ga	236	76	303	360	54	-	-	248	11	338	452	-	-	-
Ag	-	281	393	-	202	574	-	-	115	372	-	416	914	-
Rare earth elements														
Ho	-	-	41	-	-	144	70	-	-	18	-	-	58	-
Lu	1009	-	367	159	-	-	-	-	-	-	-	-		-
Nd	-	-	43	3	2	80	6	-	24	76	16	-	16	7
Ce	-	-	173	75	-	358	31	-	-	66	19	50	973	8
Y	213	-	173	170	244	213	169	633	23	317	281	87	143	47
Tb	-	-	-	-	4	116	-	37	57	89	-	-	18	-
Er	-	-	-	-	-	-	-	229	-	26	-	576	491	-
La	-	-	-	-	-	-	-	-	-	3	24	-	70	11
Toxic elements														
As	9	-	-	-	33	50	-	-	-	-	-	27	-	-
Pb	85	2901	-	-	1293	667	-	256	599	72	-	1777	1037	-
Ba	340	-	769	-	15,376	16,076	-	1976	-	1695	-	4058	3246	-
Cr	261	-	18	-	973	391	-	261	-	-	-	977	284	-
Precious metals														
Assay method	EDXRF	FA			EDXRF	FA			EDXRF	FA		EDXRF	FA	
Au	10.5	39			-	0.9			203.3	56.6		-	0.5	
Pt	-	15.3			-	-			58.7	26.7		-	-	
Pd	1.2	13.1			-	0.3			-	13.4		-	0.3	

-* Elements not detected or determined by assay; S15: LED15 strip; D15: LED15 driver; S12: LED12 strip; D12: LED12 driver; EDXRF: energy-dispersive X-ray fluorescence; AR: aqua regia digestion; 4AD: four-acid digestion; AF: alkaline fusion; FA: fire assay.

These sodium salts are soluble and stable in alkaline solution (Equation (15)), and they subsequently dissolve more readily in a mixture of nitric acid and tartaric acid [50–52]. The presence of a complexing agent, such as tartaric acid, can prevent the hydrolysis of Sn upon pH reduction (Equation (16)) [50,53]. It can also hinder the precipitation of Sn and Ti in the post-fusion acidification step (through Equations (17) and (18)) [54]. Tartaric acid can form 1:1, 1:2, and 1:4 complexes with Sn and 1:1 and 1:2 complexes with Ti [51,52].

$$Na_2SnO_3 + 3H_2O \rightarrow Na_2\,[Sn\,(OH)_6] \rightarrow Sn\,(OH)_6{}^{2-} + 2Na^+\ (pH > 12) \quad (15)$$

$$SnO_3{}^{2-} + 2H_2O \rightarrow H_2SnO_3\ (SnO_2.H_2O) \downarrow + 2OH^-\ (pH < 10) \quad (16)$$

$$Na_2SnO_3 + 2HCl + H_2O \rightarrow SnO_2.2H_2O\downarrow + 2NaCl \quad (17)$$

$$Na_2TiO_3 + 2HCl \rightarrow H_2TiO_3 \downarrow + 2NaCl \quad (18)$$

Aqua regia was unable to completely digest Ga, Ag, and REEs. GaN is a highly stable structure and is resistant to acidic digestion, which typically leads to incomplete dissolution of Ga [16,18,19]. In contrast, sodium peroxide fusion can break down refractory Ga phases in a strongly oxidizing alkaline environment, converting them into soluble sodium gallates ($NaGaO_2$), which leads to better dissolution and higher quantification of Ga in LED samples compared to AR and 4AD (Table 2) [55].

Under the analytical workflows used in this study, 4AD–ICP-OES produced higher apparent concentrations for selected REEs (Lu, Ho, Nd, Ce, and Tb) than Na_2O_2 fusion–ICP-MS (Table 2). However, because the two digests were measured using different instrumental finishes, these differences cannot be attributed solely to digestion efficiency. In a previous study on printed circuit boards, alkaline fusion with lithium borate was more effective at determining REEs than four-acid digestion [26]. The improved results of four-acid digestion here may be attributed to the greater solubility of REEs, especially Ce and Tb, in the chloride-rich medium used in four-acid digestion compared with the nitric–tartaric acid used in post-fusion leaching [56]. Furthermore, alkaline fusion treatment above 600 °C oxidizes REEs such as Ce and Tb to their (IV) oxidation states (Na_2CeO_3 and Na_2TbO_3), which are more soluble in a reductive chloride medium [23,57]. Future studies should examine the efficiency of HCl–tartaric acid for post-fusion leaching and its effect on REE determination by alkaline fusion. For Y, both digestion methods showed relatively similar results (Table 2), consistent with a previous study [17]. Utilization of $HClO_4$ in four-acid digestion aids in the solubilization of REEs by reducing the formation of insoluble fluorides (e.g., AlF_3, CaF_2) and preventing the co-precipitation of REE fluorides ($REEF_3$) [37]. All digestions, although aggressive, were deemed incomplete, as observed in LED characterization using the EPA 3052 method and other e-waste metal assays with AF [7,29]. Therefore, more optimization studies of 4AD and AF are required to better characterize the critical metals in LED waste. Additionally, the digest residues were not quantitatively recovered and weighed. Therefore, differences among digestion methods should be interpreted as recoverable concentrations under the applied digestion-measurement workflows, rather than as definitive evidence of complete dissolution or complete analyte mass balance. Future work should include residue collection, mass determination, re-digestion, and/or solid residue characterization to distinguish undissolved analyte-bearing phases from analytical or chemical losses.

For trace elements, EDXRF underreported Ga by 20–100% compared to the digestion methods (Table 2), and results for Ce, Y, Tb, Nd, and Lu were inconsistent with those from four-acid digestion (Table 2). Higher power output allows benchtop XRFs to achieve better detection limits than portable XRFs (1–5 ppm vs. >0 ppm) [37,58]. Still, EDXRF has shown limited ability to accurately determine REEs in LED lamps. Most REEs exhibit interference with one another and transition metals in X-ray signals [37]. X-ray signal overlap and

interference are reported for Mn *Kα1* and Nd *Lβ3* (5.8 eV), Ba *Lβ1* and Ce *Lα* (4.8 eV), Ga *Kα1* and Pb *Lα1* (9.2 eV), and As *Kα1* and Ga *Kβ2* (10.3 eV) [37]. *Lβ1* lines have been recommended for Pr, Nd, Sm, Gd, and Dy measurements in XRF to avoid interferences [37]. As shown in Figure 4, the concentration of precious metals (Au, Pd, Pt) was overestimated by up to 600% using EDXRF compared to the fire assay for LED samples, suggesting the unreliability of EDXRF for precious metal measurement.

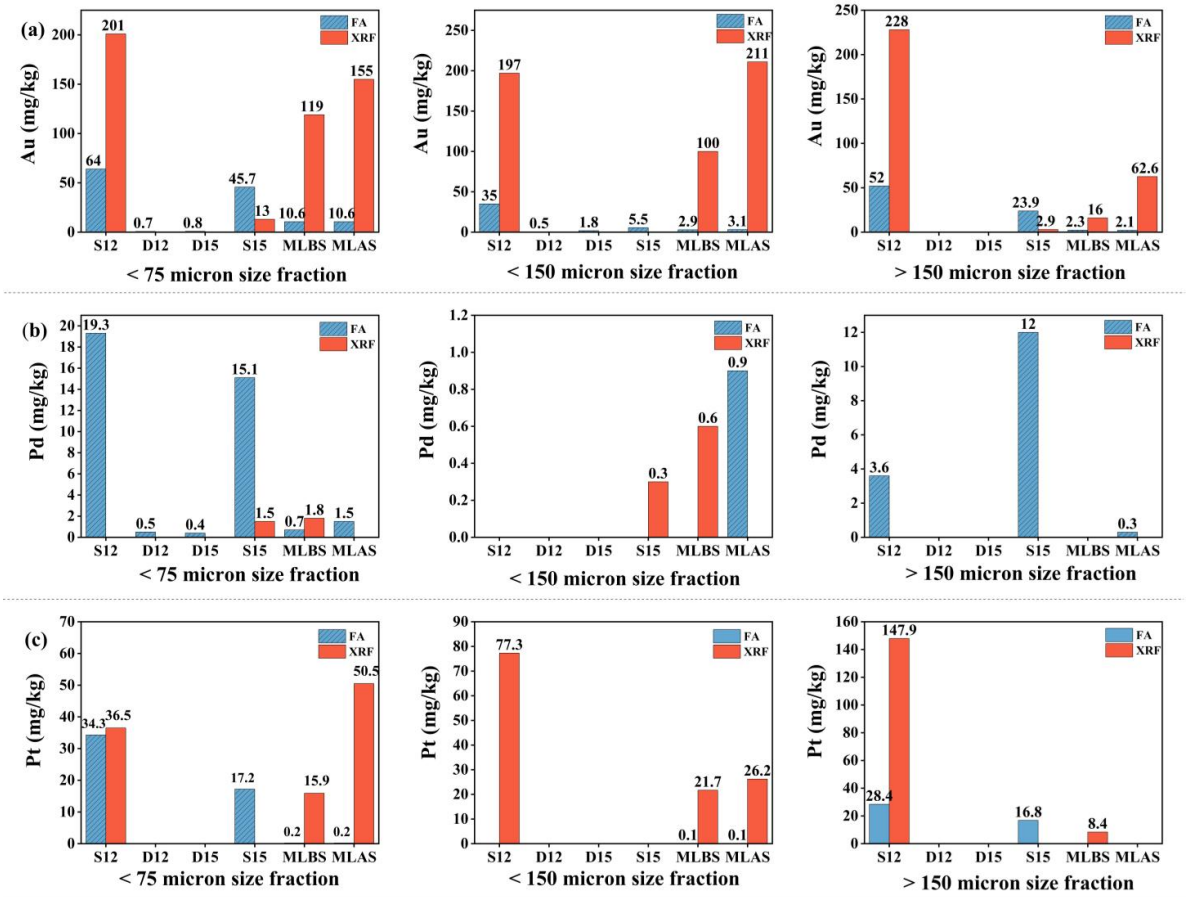


Figure 4. Comparison of fire assay (FA) and XRF method for precious metal analysis in LED samples at different size fractions. (**a**) Gold analysis comparison, (**b**) Paladium analysis comparison, (**c**) Platinum analysis comparison.

3.3.2. Tube LED Lamp Composition

Table 2 presents the total metal content of tube lamp strips and drivers (S15, S12, D15, and D12, respectively). The distribution of metals across different size fractions in the analyzed LED samples is shown in Tables S1–S6. No Ga was found in tube lamp drivers, and S12 contained higher Ga than S15 (452 mg/kg vs. 360 mg/kg). Drivers had higher REE concentrations than strips, with total REEs reaching 1076 and 2363 mg/kg in the finest size fractions of D15 and D12 samples compared to 1004 and 670 mg/kg in the finest size fractions of S15 and S12 samples (Tables S2 and S4 vs. Tables S1 and S3). The LED15 strip contained high Lu concentrations, suggesting the use of lutetium aluminum garnet (LuAG) as the phosphor material. In contrast, the LED12 strip exhibited higher levels of Tb and Y, indicating the presence of yttrium aluminum garnet (YAG) doped with Tb. Apart from Ce^{3+} utilization as a dopant in YAG phosphors, other REE ions, such as Tb^{3+}, Eu^{3+}, Ho^{3+}, Er^{3+}, and Nd^{3+}, have been used as dopants in white LED phosphors [59]. The concentrations of precious metals (Au, Pt, Pd) in tube lamp strips were considerably higher compared to their driver component (Figure 4). In the S12 sample, Au, Pt, and Pd content were 64, 34.5, and 19.3 mg/kg, respectively, in the <75 μm size fraction

(Figure 4a–c). Platinum in semiconductors is used as an ohmic contact in the form of a Ti/Pt/Au capping layer [60]. The main function of Pt in group III semiconductors is to work as a diffusion barrier, whereas Pd is mostly used as an adhesive layer to the semiconductor. Pd and Pt enhance contact stability and the uniformity of the semiconductor interface [60]. Higher concentrations of Sn, Ag, and Cu were found in the driver than in the strips for both tube lamps, corroborating a previous study [35]. It also reveals the presence of Sn-Ag-Cu solders, which are an alternative to Pb-Sn solders [17]. Other sources of Ag and Au in LED lamps include wire bonding, such as Au-Ag, Cu-Pd, and Ag-Pd [16]. An earlier study on the environmental assessment of LED manufacturing found that LED modules are composed of 59% Cu, 10% PA9T polymer, 25% silicone resin, 4% phosphor powder, 1% GaN, and 1% Au wire [10]. As shown in Table 2, a higher concentration of Al was found in the S15 sample (40%) compared to S12 (5.3%), attributed to the difficulty of separating the aluminum base from other components in LED 15T, in contrast to LED 12T. The high Si and Ca content in both lamp strips originates from class E fiberglass and organic siloxane polymers, such as polydimethylsiloxane (PDMS), which are used as encapsulants for LED chips [10,17].

3.3.3. Mixed LED Composition from Recycler Operation

The metal composition of mixed-type LED lamps before and after physical separation (MLBS, MLAS) at the recycling plant is shown in Table 3. Detailed metal content in different size fractions is presented in Tables S5 and S6. As indicated, mixed-type LEDs contain appreciable amounts of Ga, Ag, Au, and Cu, as well as valuable REEs such as Tb, even before enrichment. Table 3 shows that the physical separation process can remove substantial amounts of undesirable metals from the feedstock. For instance, Al content decreased from 38.3% to 6.6%, and Fe content decreased from 2.6% to 0.9%. Lower Al and Fe in the e-waste recycling feedstock are advantageous, as they can reduce the melting temperature during the pyrometallurgical process and reduce chemical consumption in the hydrometallurgical process [61,62]. A considerable enrichment of valuable elements, such as Ag from 345 to 985 mg/kg and Cu from 7% to 11.2%, occurred after physical separation (Table 3). The total REE concentration decreased by 15.8%, from 266 mg/kg to 224 mg/kg, after physical beneficiation (Table 3). Ga content increased by 54%, reaching 615 mg/kg after separation, and the Au concentration, which was 7.3 mg/kg before separation, showed a negligible change after metal enrichment at the industrial recycler. The concentration of toxic elements (e.g., Pb, Cr, Ba, Sb) increased significantly in mixed-type LEDs after physical separation (Table 3). For example, Pb content increased by more than three times after separation, reaching 26,531 mg/kg in the MLAS sample compared to 8412 mg/kg in the MLBS sample. Moreover, Si content increased from 6.8 to 11.9% after the enrichment process. The upgrading of toxic elements and Si has serious implications for the subsequent thermal recycling of LED lamps. The volatility of Pb at high temperatures produces toxic fumes and poses a threat to human health and the environment [61,63]. Higher Si content in e-waste recycling feedstock can lead to increased slag production, reduced furnace efficiency, and higher energy consumption during the smelting process [63,64].

Table 3. Elemental composition of LED recycler feedstock before and after physical separation process.

Elements (mg/kg)	**MLBS**				**MLAS**			
Assay Method	**EDXRF**	**AR**	**4AD**	**AF**	**EDXRF**	**AR**	**4AD**	**AF**
Al	401,106	383,367	182,721	186,641	99,979	66,894	50,855	52,782
Si	68,477	-*	-	2079	119,403	-	-	2104
Ca	53,712	7824	10,791	11,312	58,076	21,708	18,645	18,281
Fe	22,850	26,749	19,783	20,298	9514	8978	2508	2686
Strategic metals								

Table 3. *Cont.*

Elements (mg/kg)	MLBS				MLAS			
Assay Method	**EDXRF**	**AR**	**4AD**	**AF**	**EDXRF**	**AR**	**4AD**	**AF**
Cu	32,185	55,343	70,615	-	102,598	124,224	112,865	-
Sn	5117	-	-	-	37,174	-	-	2271
Ti	11,406	-	-	-	14,374	-	-	24
Ga	145	57	401	-	3	35	615	-
Ag	-	157	345	-	-	222	982	-
Rare earth elements								
Ho	-	-	16	-	-	-	29	-
Lu	-	-	-	-	842	-	-	39
Nd	-	-	49	5	62	-	27	3
Ce	-	-	19	2	141	-	78	32
Y	114	-	89	84	156	-	61	74
Tb	-	-	29	2	57	-	20	-
Er	-	-	-	-	139	-	9	84
La	-	-	-	-	-	-	-	-
Toxic elements								
As	22	-	17	-	104	-	14	-
Pb	895	8412	542	-	7125	26,531	2480	-
Ba	793	-	1579	-	2499	-	1734	-
Cr	691	-	349	-	1081	-	283	-
Precious metals								
Assay method	EDXRF	FA			EDXRF	FA		
Au	99.5	7.3			152.1	7.2		
Pt	16.5	0.1			-	0.1		
Pd	1.2	0.4			35.2	1.1		

-* Elements not detected or determined by assay; MLBS: mixed LED before physical separation; MLAS: mixed LED after separation; EDXRF: energy-dispersive X-ray fluorescence; AR: aqua regia digestion; 4AD: four-acid digestion; AF: alkaline fusion; FA: fire assay.

3.3.4. Different Size Fraction Composition

The higher concentrations of Ca and Si in the finer size fractions indicate a higher fiberglass content in the non-metal fraction, as observed during grinding of PCBs as well [38]. The inorganic components of fiberglass resins (CaO, SiO_2) are more brittle and tend to accumulate in finer fractions. At the same time, the malleability and ductility of the metallic content make it concentrate in coarser fractions, especially when impact-type crushers such as ring mills are used [38]. As illustrated in Tables S1–S6, Cu and Al concentrations are higher in the coarser fractions across different LED samples. Selective enrichment of Cu, Sn, and Al in coarser fractions during the comminution of other e-waste, such as PCBs, has also been reported [26,38,41]. Critical metals such as Ga, REEs, and Ag, as well as precious metals (Au, Pt, Pd) and toxic elements (Pb, Ba, Cr), are mostly found in finer size fractions (<75 μm) in pulverized LED lamps, which is supported by previous e-waste studies [26,32]. This phenomenon also indicates the necessity of fine crushing to liberate these metals from non-metal fractions in LED lamps, thereby facilitating leaching in later steps of the recycling process.

3.4. Precision Evaluation by Reference Materials

The accuracy of the metal assay was evaluated by performing alkaline fusion and four-acid digestion on the prepared LED reference material (denoted as EWRM) and a CRM commonly used for REE determination in ores, OREAS 465 [27], followed by recovery calculation (Table S7). In general, most recoveries were within the acceptable range (90–110%). Both methods yielded higher recoveries of Ca, Cu, and Ga with EWRM than with OREAS465. Alkaline fusion and four-acid digestion showed almost identical recoveries for Ga (98% and 99%, respectively) with EWRM. Still, AF demonstrated higher recovery for Ga than 4AD (100% vs. 93%) when OREAS465 was used as the CRM. The lowest recoveries in the four-acid digestion were observed for La, Cu, and Y at 69, 85, and 88%, respectively, which may be attributed to incomplete digestion of these elements by 4AD. The four-acid digestion showed better Ca recovery than alkaline fusion (97% vs. 89%) when using the OREAS465 CRM. In addition, Cr and Pr showed the highest positive

recovery bias with 4AD, with recoveries of 113% and 106%, respectively. Cu was not considered in EWRM for AF due to the potential loss of Cu at higher temperatures and its reaction with HBr from brominated retardant decomposition. Recovery values for most REEs in AF digestion, using OREAS465 as the CRM, were greater than 100%, possibly due to spectral line overlap in ICP-OES [26]. For instance, La recovery was 105%, while Fe recovery was 90%, suggesting interference of the Fe 379.5 nm line on the 379.478 nm line [26]. The 105–113% recoveries obtained for La, Ce, Nd, Pr, and Y in OREAS 465 suggest possible positive spectral contribution in ICP-OES analysis; however, because the CRM and LED digests differ in matrix composition and Fe/REE ratios, the magnitude of interference in the LED samples cannot be assumed to equal the CRM recovery offset. The elevated OREAS 465 recoveries are now interpreted as evidence that selected ICP-OES REE wavelengths may be susceptible to positive spectral bias and are not a universal correction factor for all LED samples. Moreover, REE concentrations determined by ICP-OES, particularly for La, Ce, Nd, Pr, and Y, should be interpreted with caution in Fe-rich matrices. Other ore reference material (RM), known as NCS DC86312, has been used for REE quantification in e-waste and can be examined for comparison with the OREAS465 results here [26]. Recovery of Cu with OREAS CRM is considerably lower than that of developed e-waste RM (80% vs. 95%). Adding similar plastic and REE phosphors to RM for waste LED is recommended as a future step to better match the original LED waste composition and improve performance for quality control [29].

In summary, Figure 5 represents why a multi-assay assessment is beneficial for LED waste characterization.

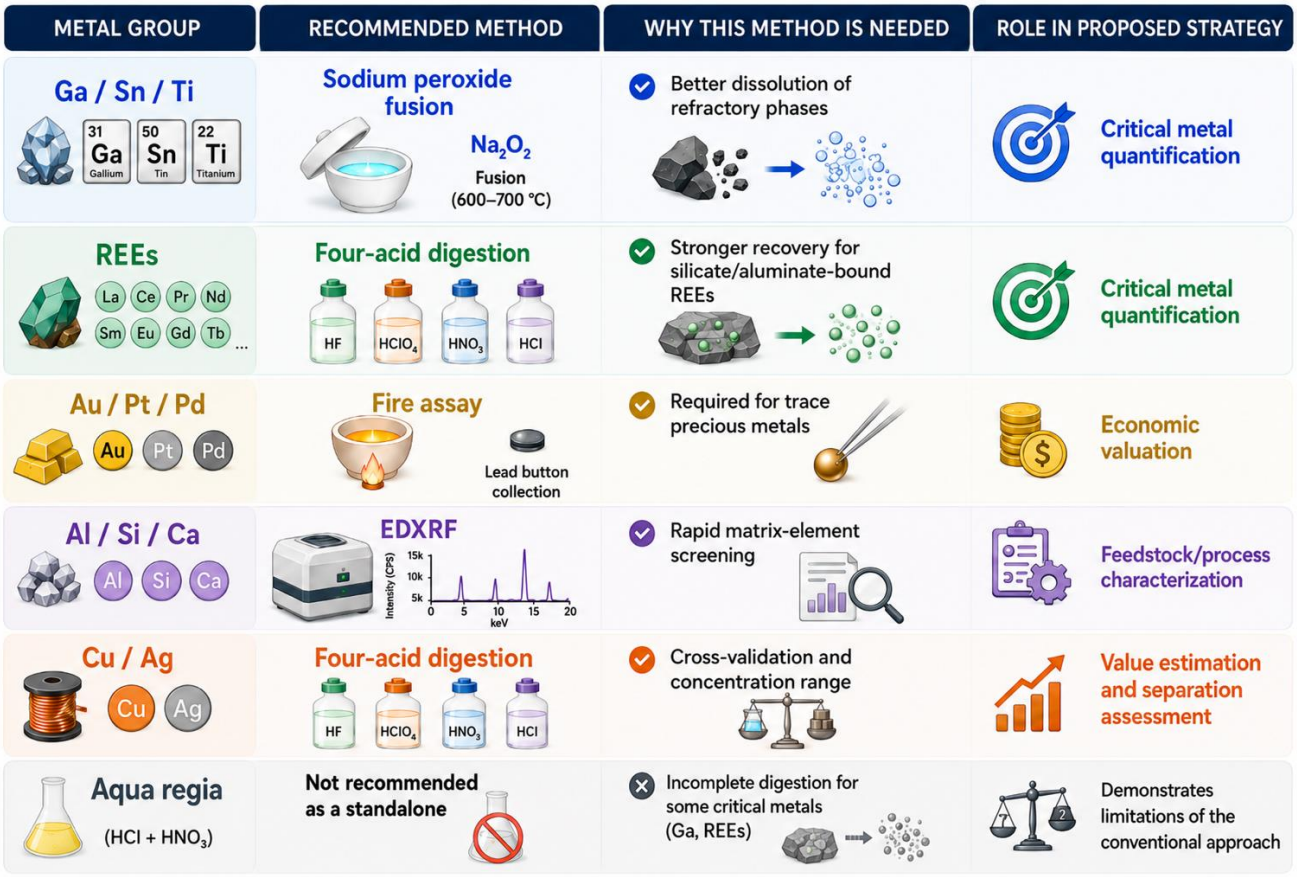


Figure 5. Comparative decision map for assay selection in LED waste characterization.

3.5. Economic Benefits of Recycling LED Lamps

The market value of different LED waste lamps is shown in Figure 6. The strip component in tube LED12T8 contained higher concentrations of precious metals such as Au, Pt, and Pd than the LED15T8 strip and therefore showed a higher intrinsic value ($11,876/t for S12 against $9070/t for S15). LED drivers (D12 and D15) have a higher metal value than LED strips; however, they constitute a smaller mass fraction of the total lamp, accounting for only 10–15% of the overall lamp value. Most of the value (56–62%) in LED strips comes from Au, followed by Cu, Pt, and Pd (Figure 6b). On the other hand, elements like Sn, Cu, and Ag are the principal value source in LED drivers (Figure 6b). Based on calculated metal concentrations in the whole tube lamp using Equation (1), the estimated values of waste LED15T8 and LED12T8 are $2094 and $1649 per tonne, respectively, with most of the value originating from the LED strip component (Figure 6c). These results align with previous findings, which reported an approximate value of $2406 per tonne for tubular LED lamps [35].

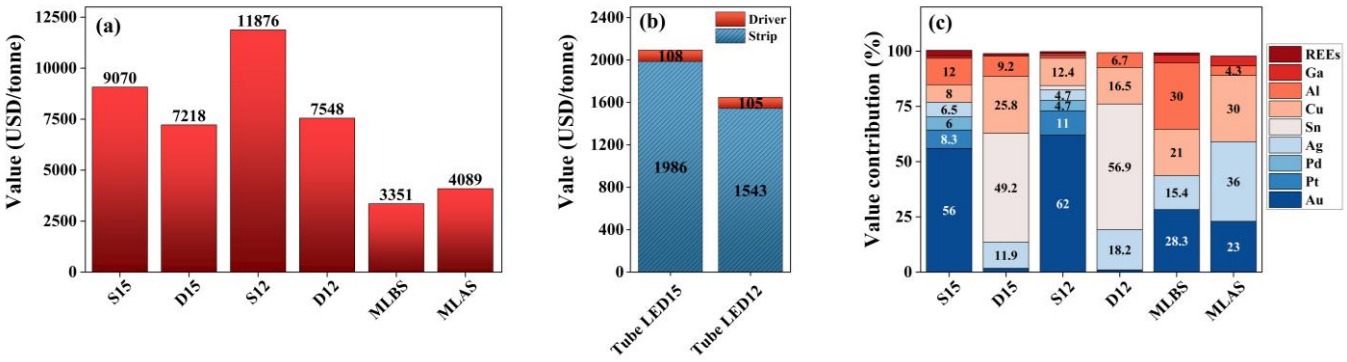


Figure 6. Monetary value in recycling LED lamps. (**a**) Economic value of different LED samples; (**b**) tube LED lamp components' contributions to total value; (**c**) contributions of different metals to value in studied LED samples.

Interestingly, the metal value in shredded mixed LED lamps before physical separation (MLBS) is higher than that of tube lamp strips, at $3351/t, and increases to $4089/t with physical separation (MLAS), indicating a considerable economic return from recycling. Au, Cu, Sn, Ag, and Al are the primary contributors to metal value in mixed LEDs (Figure 6b). Interestingly, Al accounts for 30% of the value in mixed LED waste before physical separation, whereas after physical separation, Ag and Cu become the primary value sources at 36% and 30%, respectively (Figure 6c). High concentrations of Ag have been reported in various components of LED lamps (Table 1). Although the contribution of critical metals such as Ga and REEs to the economic value of waste LEDs is minimal, the coexistence of precious metals aids in the economic recovery of Ga and REEs from LED lamps. Therefore, recycling Ga and REEs from waste LEDs should be prioritized as a secondary source. According to the latest government reports on LED lamp sales and collection in British Columbia, Canada, more than 8,920,000 LED lamps were sold in 2024, and 903,000 end-of-life LED units were collected [65]. Given that each lamp weighs approximately 200 g, this corresponds to about 1250 tonnes of in-use (in-stock) LEDs and 180 tonnes of end-of-life LEDs. Using the metal composition data from industrial recycler samples (MLBS) and their corresponding value of $3351 per tonne, the estimated total value of in-use and end-of-life LEDs in British Columbia in 2024 is approximately $4.18 and $0.6 million USD, respectively.

3.6. Environmental Benefits of Recycling LED Lamps

The potential environmental benefit of avoiding rock excavation through the recycling of end-of-life LED lamps is shown in Figure 7a. Since e-waste, including LED lamps, contains substantially higher concentrations of critical metals than primary ores [66], recycling can yield substantial environmental benefits. For instance, recycling a tonne of tube LED strips can obviate the need to excavate 194–309 tonnes of rock by primary mining (Figure 7a). Elements such as Au, Cu, Pt, and Pd in LED strips (Figure 7c) provide the highest environmental return. Recycling LED drivers (D12, D15) can yield higher environmental credit than recycling strips (S12, S15), thereby avoiding 341–363 tonnes of ore mining. As shown in Figure 7c, Sn and Cu are among the highest contributors to environmental gain from recycling LED drivers, with shares of more than 66% and 28%, respectively. The environmental benefit of recycling a complete tube lamp is much lower than that of metal-rich components (strip and driver), reporting 47.6 and 45.4 tonnes of avoided rock mining per tonne of tube lamp. However, estimates indicate that mixed LED waste from the industrial recycler (MLBS) can offer nearly 60% greater ecological advantage than tube lamps, thereby preventing 75.5 tonnes of rock excavation. This number increases by 57% with the physical separation process (MLAS), reaching 118.5 tonnes of land disturbance prevented. Figure 7c shows that Ag, Au, and Cu contribute the most to the mixed-type LED samples from the industrial recycler. Recycling all the LED lamps collected in British Columbia in 2024 (903,000 units, 180 tonnes) can provide a 13.5 kt avoided rock excavation benefit. Life cycle assessment (LCA) studies have shown that loading, hauling, and comminution, which are directly related to the volume of excavated ore, are major contributors to greenhouse gas (GHG) emissions during the mining of iron ore, bauxite, and copper ore [67]. Therefore, rock excavation reduction is directly linked to reductions in overall GHG emissions, energy consumption, and the environmental impact of the metal supply chain [67]. Recycling LED lamps is therefore indispensable for energy conservation and environmental protection, and mining companies can reduce their overall emissions by supporting recycling companies and leveraging the environmental credits generated by recycling.

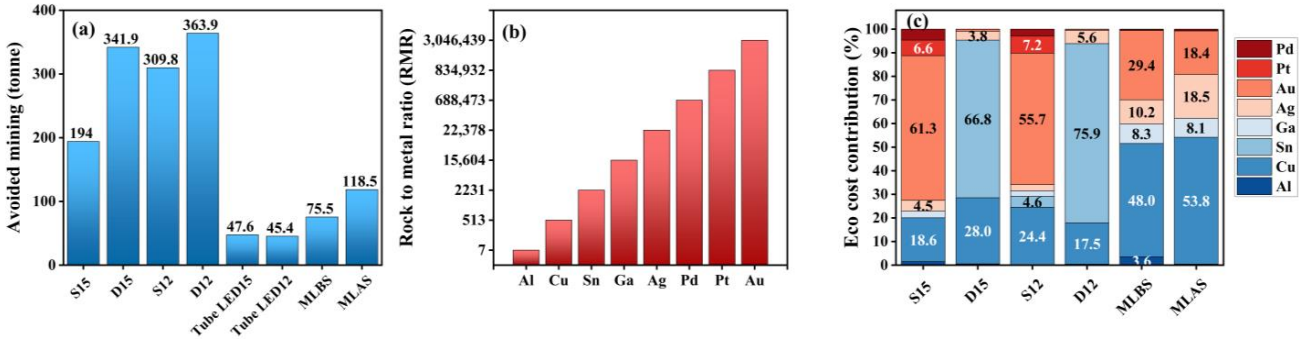


Figure 7. Environmental benefit from recycling LED lamps. (**a**) Prevented tonnes of rock excavation in mining by recycling a tonne of LED samples; (**b**) tonne of waste rock extraction required to mine different metals; (**c**) contribution of different metals in LED lamps to the environmental impact of mining.

4. Conclusions

This study developed a practical framework for evaluating LED waste recycling under industrially relevant conditions by integrating recyclability assessment, metal characterization, and environmental benefit analysis. The recyclability analysis showed that non-standardized lamp designs, particularly in tube LED lamps, can complicate manual dismantling and grinding, highlighting the importance of design for recycling in future

product development. Comparison of digestion methods showed that aqua regia is inadequate for quantifying Ga and REEs in LED waste, while alkaline fusion showed better accuracy for Ga, Sn, and Ti, and four-acid digestion recovered higher amounts of REEs, Cu, and Ag under the conditions used in this study. EDXRF was also effective for the rapid determination of major elements such as Si, Al, and Ca. These findings indicate that no single assay method is sufficient to fully characterize LED waste, and further optimization of alkaline fusion and four-acid digestion is required.

Metal assay results further showed that LED drivers contained higher concentrations of Cu, Sn, Ag, and REEs, whereas Ga, Au, Pt, and Pd were detected only in the strip component, emphasizing the importance of component-specific characterization for recycling strategy development. Overall, this work demonstrates that combining detailed metal analysis with RMR-based environmental assessment provides a useful decision-support framework for quantifying the environmental value of urban mining. Although REEs were excluded from the present RMR calculation due to the lack of available RMR data, their inclusion in future studies is expected to increase the estimated environmental benefits of LED recycling. More broadly, the transferability of the RMR approach to other e-waste streams underscores its potential as a tool to guide recycling strategies that reduce the environmental burden of primary metal production.

Supplementary Materials: The following supporting information can be downloaded at: https://www.mdpi.com/article/10.3390/recycling11070120/s1, Figure S1: Wide variation in designs of tube lamps. (a) disassembled LED 12T8 and (b) disassembled LED15T8. (c) LED12T8 strip, (d) LED15T8 strip, (e) LED12T8 driver, (f) LED15T8 driver. (g) weight distribution of components in two models of tube lamp. Each lamp weighed approximately 200 g; Figure S2: Comparison of grindability for different LED samples in the study; Table S1: Metal composition of LED 15T8 strip in different size fractions and digestion methods; Table S2: Metal composition of LED 15T8 driver in different size fractions and digestion methods; Table S3: Metal composition of LED 12T8 strip in different size fractions and digestion methods; Table S4: Metal composition of LED 12T8 driver in different size fractions and digestion methods; Table S5: Metal composition of LEDs before separation at different size fractions and digestion methods; Table S6: Metal composition of LEDs after separation at different size fractions and digestion methods; Table S7: Certified reference material (CRM) evaluation; Text S1: Detailed grinding procedure.

Author Contributions: M.G.-A.: Conceptualization, Investigation, Methodology, Writing—original draft, Writing—review and editing, Project administration. M.H.: Writing—review and editing, Supervision, Funding acquisition, Project administration. All authors have read and agreed to the published version of the manuscript.

Funding: This research was funded by the Natural Sciences and Engineering Research Council of Canada (NSERC), grant number ALLRP 586647-2023.

Data Availability Statement: Data are available upon request. Further inquiries can be directed at the corresponding author.

Acknowledgments: We acknowledge the support of the Natural Sciences and Engineering Research Council of Canada (NSERC) [funding reference number ALLRP 586647-2023]. The author would like to acknowledge the financial support provided by Maria Holuszko at the University of British Columbia. The author also acknowledges the help of Ahmed Bouajila from Impact Global Solutions (IGS) Inc. in providing expert advice and necessary technical details, and Contact Environmental Inc. for an in-kind contribution in the form of LED lamp samples, expert advice, and other necessary technical details. BC Electrical Inc. is also acknowledged for providing unprocessed waste LEDs from their industrial operations for our characterization study. We greatly appreciate their efforts in consistently delivering these samples on time.

Conflicts of Interest: The authors declare no conflicts of interest.

Abbreviations

The following abbreviations are used in this manuscript:

LED	Light-emitting diode
GaN	Gallium nitride
InGaN	Indium gallium nitride
YAG	Yttrium aluminum garnet
LuAG	Lutetium aluminum garnet
REE	Rare earth element
PCB	Printed circuit board
RMR	Rock-to-metal ratio
LMFP	Lithium manganese iron phosphate
SMD	Surface-mounted device
CI	Crushability index
ISI	Impact strength index
MLBS	Mixed LED before separation
MLAS	Mixed LED after separation
AR	Aqua regia
4AD	Four-acid digestion
AF	Alkaline fusion
FA	Fire assay
EDXRF	Energy-dispersive X-ray fluorescence
RM	Reference material
LOD	Limit of detection
EWRM	E-waste reference material
PDMS	Polydimethylsiloxane

References

1. Qiu, Y.; Suh, S. Economic Feasibility of Recycling Rare Earth Oxides from End-of-Life Lighting Technologies. *Resour. Conserv. Recycl.* **2019**, *150*, 104432. [CrossRef]
2. Mizanur Rahman, S.M.; Kim, J.; Lerondel, G.; Bouzidi, Y.; Nomenyo, K.; Clerget, L. Missing Research Focus in End-of-Life Management of Light-Emitting Diode (LED) Lamps. *Resour. Conserv. Recycl.* **2017**, *127*, 256–258. [CrossRef]
3. ProductCare. LightRecycle Annual Report. Available online: https://www2.gov.bc.ca/assets/gov/environment/waste-management/recycling/recycle/lighting-pcr/pca_lights_annual_and_assurance_reports_2012.pdf (accessed on 4 July 2026).
4. ProductCare. LightRecycle Annual Report. Available online: https://www2.gov.bc.ca/assets/gov/environment/waste-management/recycling/recycle/lighting-pcr/pcr_lights_annual_and_assurance_reports_2020.pdf (accessed on 4 July 2026).
5. Jia, J.; Zhang, A.; Li, D.; Liu, X.; Xu, B.; Jia, H. Preparation and Properties of the Flexible Remote Phosphor Film for Blue Chip-Based White LED. *Mater. Des.* **2016**, *102*, 8–13. [CrossRef]
6. Sideris, K.M.; Katsiris, I.; Fragkoulis, D.; Stathopoulos, V.N.; Sinioros, P. Waste SMD LEDs from End-of-Life Residential LED Lamps: Presence and Characterisation of Rare Earth Elements and Precious Metals as a Function of Correlated Colour Temperature. *Recycling* **2024**, *9*, 128. [CrossRef]
7. Oliveira, R.P.; Botelho Junior, A.B.; Espinosa, D.C.R. *Characterization of Wasted LEDs from Tubular Lamps Focused on Recycling Process by Hydrometallurgy*; Springer: Berlin/Heidelberg, Germany, 2020; pp. 317–325.
8. Ku, A.Y.; Setlur, A.A.; Loudis, J. Impact of Light Emitting Diode Adoption on Rare Earth Element Use in Lighting: Implications for Yttrium, Europium, and Terbium Demand. *Electrochem. Soc. Interface* **2015**, *24*, F04154. [CrossRef]
9. Illés, I.B.; Kékesi, T. A Comprehensive Aqueous Processing of Waste LED Light Bulbs to Recover Valuable Metals and Compounds. *Sustain. Mater. Technol.* **2023**, *35*, e00572. [CrossRef]
10. Gao, W.; Zeng, X.; Yang, H.; Chen, F.; Pan, A.; Yang, F.; Wang, Y.; Li, H.; Ren, Z.; Zhang, G.; et al. Green Manufacturing Evaluation of Light-Emitting Diodes Lamps Production: Resource and Environmental Assessment. *Renew. Sustain. Energy Rev.* **2025**, *211*, 115317. [CrossRef]
11. Cenci, M.P.; Dal Berto, F.C.; Camargo, P.S.S.; Veit, H.M. Separation and Concentration of Valuable and Critical Materials from Wasted LEDs by Physical Processes. *Waste Manag.* **2021**, *120*, 136–145. [CrossRef] [PubMed]
12. Mir, S.; Vaishampayan, A.; Dhawan, N. A Review on Recycling of End-of-Life Light-Emitting Diodes for Metal Recovery. *Jom* **2022**, *74*, 599–611. [CrossRef]

13. Alonso, E.; Brioche, A.S.; Schulte, R.; Trimmer, L.M.; Kim, J.-E.; Gulley, A.L.; Pineault, D.G. *World Minerals Outlook—Cobalt, Gallium, Helium, Lithium, Magnesium, Palladium, Platinum, and Titanium Through 2029*; Scientific Investigations Report; USGS: Reston, VA, USA, 2025.
14. Nassar, N.T.; Pineault, D.; Allen, S.M.; McCaffrey, D.M.; Padilla, A.J.; Brainard, J.L.; Bayani, M.; Shojaeddini, E.; Ryter, J.W.; Lincoln, S.; et al. *Methodology and Technical Input for the 2025 U.S. List of Critical Minerals—Assessing the Potential Effects of Mineral Commodity Supply Chain Disruptions on the U.S. Economy*; Open-File Report; USGS: Reston, VA, USA, 2025.
15. Nassar, N.T.; Lederer, G.W.; Brainard, J.L.; Padilla, A.J.; Lessard, J.D. Rock-to-Metal Ratio: A Foundational Metric for Understanding Mine Wastes. *Environ. Sci. Technol.* **2021**, *56*, 6710–6721. [CrossRef] [PubMed]
16. Mandal, S.; Binti Bakaruddin, B.R.; Jeon, S.; Lee, Y.; Kim, K.W. Assessment of the Recycling Potential of Valuable Metals by Mapping the Elemental Composition in Discarded Light-Emitting Diodes (LEDs). *J. Environ. Manag.* **2023**, *328*, 116900. [CrossRef] [PubMed]
17. Vinhal, J.T.; de Oliveira, R.P.; Coleti, J.L.; Espinosa, D.C.R. Characterization of End-of-Life LEDs: Mapping Critical, Valuable and Hazardous Elements in Different Devices. *Waste Manag.* **2022**, *151*, 113–122. [CrossRef] [PubMed]
18. Zamprogno Rebello, R.; Weitzel Dias Carneiro Lima, M.T.; Yamane, L.H.; Ribeiro Siman, R. Characterization of End-of-Life LED Lamps for the Recovery of Precious Metals and Rare Earth Elements. *Resour. Conserv. Recycl.* **2020**, *153*, 104557. [CrossRef]
19. Kumar, A.; Kuppusamy, V.K.; Holuszko, M.; Song, S.; Loschiavo, A. LED Lamps Waste in Canada: Generation and Characterization. *Resour. Conserv. Recycl.* **2019**, *146*, 329–336. [CrossRef]
20. Bonin, M.; Fontaine, F.G.; Larivière, D. Comparative Studies of Digestion Techniques for the Dissolution of Neodymium-Based Magnets. *Metals* **2021**, *11*, 1149. [CrossRef]
21. Liu, H.; Zhang, S.; Pan, D.; Tian, J.; Yang, M.; Wu, M.; Volinsky, A.A. Rare Earth Elements Recycling from Waste Phosphor by Dual Hydrochloric Acid Dissolution. *J. Hazard. Mater.* **2014**, *272*, 96–101. [CrossRef] [PubMed]
22. Liang, Y.; Liu, Y.; Lin, R.; Guo, D.; Liao, C. Leaching of Rare Earth Elements from Waste Lamp Phosphor Mixtures by Reduced Alkali Fusion Followed by Acid Leaching. *Hydrometallurgy* **2016**, *163*, 99–103. [CrossRef]
23. Xie, B.; Liu, C.; Wei, B.; Wang, R.; Ren, R. Recovery of Rare Earth Elements from Waste Phosphors via Alkali Fusion Roasting and Controlled Potential Reduction Leaching. *Waste Manag.* **2023**, *163*, 43–51. [CrossRef] [PubMed]
24. Guo, X.; Liu, J.; Qin, H.; Liu, Y.; Tian, Q.; Li, D. Recovery of Metal Values from Waste Printed Circuit Boards Using an Alkali Fusion-Leaching-Separation Process. *Hydrometallurgy* **2015**, *156*, 199–205. [CrossRef]
25. Kebbekus, B.B. Preparation of Samples for Metals Analysis. In *Sample Preparation Techniques in Analytical Chemistry*; Wiley: Hoboken, NJ, USA, 2003; pp. 227–270.
26. Makombe, M.; van der Horst, C.; Somerset, V. Improved Borate Fusion Technique for Determination of Rare Earth Elements in Electronic Waste Components. *Environ. Technol.* **2023**, *44*, 1047–1060. [CrossRef] [PubMed]
27. Helmeczi, E.; Wang, Y.; Brindle, I.D. A Novel Methodology for Rapid Digestion of Rare Earth Element Ores and Determination by Microwave Plasma-Atomic Emission Spectrometry and Dynamic Reaction Cell-Inductively Coupled Plasma-Mass Spectrometry. *Talanta* **2016**, *160*, 521–527. [CrossRef] [PubMed]
28. Qi, T.; Yang, X.; Liu, Y.; Wen, H.; Liu, F.; Yue, Z.; Qi, Z.; Zhang, H.; Fu, J.; Liu, Q.; et al. High-Precision Analysis of Toxic Metals in Lithium-Ion Battery Materials across Various Complex Media. *Anal. Chim. Acta* **2024**, *1331*, 343334. [CrossRef] [PubMed]
29. Van Yken, J.; Cheng, K.Y.; Boxall, N.J.; Sheedy, C.; Nikoloski, A.N.; Moheimani, N.R.; Kaksonen, A.H. A Comparison of Methods for the Characterisation of Waste-Printed Circuit Boards. *Metals* **2021**, *11*, 1935. [CrossRef]
30. Zhou, J.; Zhu, N.; Liu, H.; Wu, P.; Zhang, X.; Zhong, Z. Recovery of Gallium from Waste Light Emitting Diodes by Oxalic Acidic Leaching. *Resour. Conserv. Recycl.* **2019**, *146*, 366–372. [CrossRef]
31. Zhan, L.; Wang, Z.; Zhang, Y.; Xu, Z. Recycling of Metals (Ga, In, As and Ag) from Waste Light-Emitting Diodes in Sub/Supercritical Ethanol. *Resour. Conserv. Recycl.* **2020**, *155*, 104695. [CrossRef]
32. Zhang, A.; Li, S.; Zhuang, X.; Song, X.; Gu, W.; Bai, J.; Wang, J. Separation and Recycling of Au and Ag from Waste Light-Emitting Diodes. *Environ. Technol.* **2024**, *45*, 3004–3015. [CrossRef] [PubMed]
33. Pourhossein, F.; Mousavi, S.M. Enhancement of Copper, Nickel, and Gallium Recovery from LED Waste by Adaptation of Acidithiobacillus Ferrooxidans. *Waste Manag.* **2018**, *79*, 98–108. [CrossRef] [PubMed]
34. Lim, S.R.; Kang, D.; Ogunseitan, O.A.; Schoenung, J.M. Potential Environmental Impacts of Light-Emitting Diodes (LEDs): Metallic Resources, Toxicity, and Hazardous Waste Classification. *Environ. Sci. Technol.* **2011**, *45*, 320–327. [CrossRef] [PubMed]
35. Cenci, M.P.; Dal Berto, F.C.; Schneider, E.L.; Veit, H.M. Assessment of LED Lamps Components and Materials for a Recycling Perspective. *Waste Manag.* **2020**, *107*, 285–293. [CrossRef] [PubMed]
36. Oleszek, S.; Grabda, M.; Shibata, E.; Nakamura, T. Distribution of Copper, Silver and Gold during Thermal Treatment with Brominated Flame Retardants. *Waste Manag.* **2013**, *33*, 1835–1842. [CrossRef] [PubMed]
37. Potts, P.J. *A Handbook of Silicate Rock Analysis*; Springer: Boston, MA, USA, 1992.
38. Abbadi, A.; Rácz, Á.; Bokányi, L. Exploring the Comminution Process of Waste Printed Circuit Boards in Recycling: A Review. *J. Mater. Cycles Waste Manag.* **2024**, *26*, 1326–1348. [CrossRef]

39. Toraman, O.Y.; Kahraman, S.; Cayirli, S. Predicting the Crushability of Rocks from the Impact Strength Index. *Miner. Eng.* **2010**, *23*, 752–754. [CrossRef]
40. Nikolić, V.; Ferradal, P.S.; Medina Pierres, J.; Menéndez-Aguado, J.M.; Trumić, M. Methods for Estimating the Bond Work Index for Ball Mills. *Minerals* **2024**, *14*, 1264. [CrossRef]
41. Rudnik, E. Innovative Approaches to Tin Recovery from Low-Grade Secondary Resources: A Focus on (Bio)Hydrometallurgical and Solvometallurgical Methods. *Materials* **2025**, *18*, 819. [CrossRef] [PubMed]
42. Andrade, D.F.; Machado, R.C.; Bacchi, M.A.; Pereira-Filho, E.R. Proposition of Electronic Waste as a Reference Material-Part 1: Sample Preparation, Characterization and Chemometric Evaluation. *J. Anal. At. Spectrom.* **2019**, *34*, 2394–2401. [CrossRef]
43. Remeteiová, D.; Ružičková, S.; Mičková, V.; Laubertová, M.; Slezáková, R. Evaluation of Us Epa Method 3052 Microwave Acid Digestion for Quantification of Majority Metals in Waste Printed Circuit Boards. *Metals* **2020**, *10*, 1511. [CrossRef]
44. Twyman, R.M. Sample Dissolution for Elemental Analysis | Wet Digestion. In *Encyclopedia of Analytical Science*; Elsevier: Amsterdam, The Netherlands, 2005; pp. 146–153.
45. Robinson, P. Handbook of Rock and Mineral Analysis Chapter 2 (Part 1) Analysis of Geological Materials—1: Sample Preparation Methods. *Geostand. Geoanal. Res.* **2025**, *49*, 9–50. [CrossRef]
46. Hu, Z.; Qi, L. Sample Digestion Methods. In *Treatise on Geochemistry*, 3rd ed.; Elsevier: Amsterdam, The Netherlands, 2013; Volume 15, pp. 87–109.
47. Brewer, L. The Thermodynamic Properties of the Oxides and Their Vaporization Processes. *Chem. Rev.* **1953**, *52*, 1–75. [CrossRef]
48. Rafter, T.A. Sodium Peroxide Decomposition of Minerals in Platinum Vessels. *Analyst* **1950**, *75*, 485. [CrossRef]
49. Fosu, A.Y.; Bartier, D.; Diot, F.; Kanari, N. Insight into the Extractive Metallurgy of Tin from Cassiterite. *Materials* **2024**, *17*, 3312. [CrossRef] [PubMed]
50. Zhang, Y.; Su, Z.; Liu, B.; You, Z.; Yang, G.; Li, G.; Jiang, T. Sodium Stannate Preparation from Stannic Oxide by a Novel Soda Roasting-Leaching Process. *Hydrometallurgy* **2014**, *146*, 82–88. [CrossRef]
51. EPA, U.; Protection Division, R. *MARLAP Manual Volume II: Chapter 13, Sample Dissolution*; U.S. EPA: Washington, DC, USA, 2004.
52. Mattock, G. The Complex-Forming Behaviour of Tin, Germanium, and Titanium with Some Dibasic Carboxylic Acids. *J. Chem. Soc.* **1954**, *157*, 989–997. [CrossRef]
53. Yang, D.; Wu, Z.; Ren, K.; Dong, P.; Zhang, D.; Yang, B.; Liang, F. Recent Advances of the Thermodynamic Behavior of Tin Species in Aqueous Solution. *J. Min. Metall. Sect. B Metall.* **2023**, *59*, 1–15. [CrossRef]
54. Suri, A.K.; Subramanian, C.; Gupta, C.K. Investigations on Flowsheet Development for the Treatment of Niobium-Tantalum Bearing Cassiterite. *Miner. Process. Extr. Metall. Rev.* **1992**, *9*, 293–303. [CrossRef]
55. Chen, W.S.; Hsu, L.L.; Wang, L.P. Recycling the GaN Waste from LED Industry by Pressurized Leaching Method. *Metall.* **2018**, *8*, 861. [CrossRef]
56. Özkan, A.B.; Birol, B.; Sönmez, M.Ş. Selective Recovery of Y-Eu and Tb-La-Ce Oxides from Fluorescent Lamp Waste Using a Two-Step Conventional and Microwave-Assisted Hydrometallurgical Process. *J. Sustain. Metall.* **2025**, *11*, 2283–2299. [CrossRef]
57. Sinha, M.K.; Tanvar, H.; Mishra, B. Hydrometallurgical Recovery of Critical Metal Values from Heterogeneous Trichromatic Phosphor Waste. *J. Sustain. Metall.* **2025**, *11*, 3575–3589. [CrossRef]
58. Specht, A.J.; Adesina, K.E.; Read, D.E.; Weisskopf, M.G. Benchtop X-Ray Fluorescence to Quantify Elemental Content in Nails Non-Destructively. *Sci. Total Environ.* **2024**, *918*, 170601. [CrossRef] [PubMed]
59. Gao, S.; Pan, Y.; Jia, K.; Pan, H.; Xiong, Y.; Cheng, S. Nanocrystalline Y3Ga5O12:Eu3+,Tb3+: A Promising Phosphor for White LED Lighting Application. *ACS Appl. Nano Mater.* **2024**, *7*, 20094–20100. [CrossRef]
60. Ivey, D.G. Platinum Metals in Ohmic Contacts to III-V Semiconductors. *Platin. Metall. Rev.* **1999**, *43*, 2–12. [CrossRef]
61. Wan, X.; Zhou, L.; Chen, Z.; Shen, L.; Chen, M. Review on Pyrometallurgical Smelting Options for Recycling Precious and Platinum Group Metals from Secondary Resources. In *Metallurgical and Materials Transactions B: Process Metallurgy and Materials Processing Science*; Springer: Berlin/Heidelberg, Germany, 2025.
62. Islam, M.K.; Somerville, M.; Pownceby, M.I.; Tardio, J.; Haque, N.; Bhargava, S. Deportment of Metals from E-Waste PCBs towards Alloy and Slag Phases during Smelting Using CaO-Al_2O_3-SiO_2-B_2O_3 Slags. *Minerals* **2023**, *13*, 727. [CrossRef]
63. Faraji, F.; Golmohammadzadeh, R.; Pickles, C.A. Potential and Current Practices of Recycling Waste Printed Circuit Boards: A Review of the Recent Progress in Pyrometallurgy. *J. Environ. Manag.* **2022**, *316*, 115242. [CrossRef]
64. Isaksson, J.; Samuelsson, C.; Lennartsson, A.; Andersson, A. *Settling Mechanisms of Valuable Metal Droplets in Iron Silicate Slag, Luleå*; LTU: Luleå, Sweden, 2023.
65. ProductCare. *British Columbia Lamps and Lighting Equipment Extended Producer Responsibility Program*; Product Care Association of Canada: Vancouver, BC, Canada, 2024.

66. Golzar-Ahmadi, M.; Bahaloo-Horeh, N.; Pourhossein, F.; Norouzi, F.; Schoenberger, N.; Hintersatz, C.; Chakankar, M.; Holuszko, M.; Kaksonen, A.H. Pathway to Industrial Application of Heterotrophic Organisms in Critical Metals Recycling from E-Waste. *Biotechnol. Adv.* **2024**, *77*, 108438. [CrossRef] [PubMed]
67. Norgate, T.; Haque, N. Energy and Greenhouse Gas Impacts of Mining and Mineral Processing Operations. *J. Clean. Prod.* **2010**, *18*, 266–274. [CrossRef]

Disclaimer/Publisher's Note: The statements, opinions and data contained in all publications are solely those of the individual author(s) and contributor(s) and not of MDPI and/or the editor(s). MDPI and/or the editor(s) disclaim responsibility for any injury to people or property resulting from any ideas, methods, instructions or products referred to in the content.